Short title: Genetic basis of water use efficiency in canola

Multi-environment QTL analysis delineates a major locus associated with homoeologous exchanges for water-use efficiency and seed yield in allopolyploid *Brassica napus*

Harsh Raman[1*], Rosy Raman[1], Ramethaa Pirathiban[2], Brett McVittie[1], Niharika Sharma[3], Shengyi Liu[4], Yu Qiu[1], Anyu Zhu[5], Andrzej Killian[5], Brian Cullis[2], Graham D. Farquhar[6], Hilary S. Williams[6], Rosemary White[7], David Tabah[8] Andrew Easton[8] and Yuanyuan Zhang[4*]

[1]NSW Department of Primary Industries, Wagga Wagga Agricultural Institute, Wagga Wagga, NSW 2650, Australia
[2]Centre for Biometrics and Data Science for Sustainable Primary Industries, National Institute for Applied Statistics Research Australia, University of Wollongong NSW 2522, Australia
[3]NSW Department of Primary Industries, Orange Agricultural Institute, ORANGE, NSW 2800, Australia

[4]Oil Crops Research Institute, Chinese Academy of Agricultural Sciences, Wuhan, Hubei, 430062, China

[5] Diversity Arrays Technology P/L, University of Canberra, ACT 2601, Australia

[6]Research School of Biology, Australian National University, Canberra ACT 2601, Australia
[7]CSIRO, Canberra, ACT 2601, Australia
[8]Advanta Seeds Pty Ltd, 268 Anzac Avenue, Toowoomba, QLD 4350, Australia

Date of submission: 9th July 2021

Number of tables: 1

Figures: 6

Word count (start of the introduction to the end of the acknowledgements): 6475

Supplementary figures: 3

Supplementary tables: 15

Corresponding authors:

Harsh Raman
NSW Department of Primary Industries
Wagga Wagga Agricultural Institute, PMB, WAGGA WAGGA, NSW 2650, Australia
Tel: +61269381925
Email: harsh.raman@dpi.nsw.gov.au

Yuanyuan Zhang
Oil Crops Research Institute,
Chinese Academy of Agricultural Sciences, , Wuhan, Hubei 430062, China
Email: zhangyy@caas.cn

Summary

- Canola varieties exhibit discernible variation in drought avoidance and drought escape traits, suggesting its adaptation to water-deficit environments. However, the underlying mechanisms are poorly understood.
- A doubled haploid (DH) population was analysed to identify QTL associated with water use efficiency (WUE) related traits. Based on the resequenced parental genome data, we developed sequence-capture based markers for fine mapping. mRNA-Seq was performed to determine the expression of candidate genes underlying QTL for carbon isotope discrimination ($\Delta^{13}C$).
- QTL contributing to main and QTL × Environment interaction effects for $\Delta^{13}C$ and for agronomic WUE were identified. One multi-trait QTL for $\Delta^{13}C$, days to flower, plant height and seed yield was identified on chromosome A09, in the vicinity of *ERECTA*. Interestingly, this QTL region was overlapped with a homoeologous exchange event (HE), suggesting its association with the major QTL. Transcriptome analysis revealed several differentially expressed genes between parental lines, including in HE regions.
- This study provides insights into the complexity of WUE related genes in the context of canola adaptation to water-deficit conditions. Our results suggest that alleles for high $\Delta^{13}C$ contribute positively to canola yield. Genetic and genomic resources developed herein could be utilised to make genetic gains for improving canola WUE.

Key words: water use efficiency, carbon isotope discrimination, drought avoidance, genetic analysis, physiology, yield

Introduction

Drought is the major abiotic stress that reduces the yield potential of various crops, especially in arid and semi-arid regions, of which 89% of regions are prevalent in Oceania (Koohafkan & Stewart, 2008). No doubt the impact of drought stress on crop productivity can be alleviated through irrigation at the 'critical' stages of plant development. However, in recent years fresh water, suitable for irrigation, is becoming scarce for crop production, required to meet the demand of a burgeoning human population (Gleick, 2000). Predicted climatic patterns such as debilitating drought and heat-wave episodes and their possible increased frequency further pose a significant threat to crop production (Smith & De Smet, 2012; Mills et al., 2018). The proportion of arable land per capita is also decreasing at a significant rate due to population growth and land degradation (http://www.fao.org/sustainability/). Therefore, improving crop varieties that have high yield potential and utilise water more effectively or require less water could provide a part of the solution to reduce the negative impacts of drought stress and increase productivity and food security (Passioura, 1977; Kijne et al., 2003; Blum, 2009; Bertolino et al., 2019; Leakey et al., 2019).

In nature, to cope with water-deficit conditions, plants have evolved different strategies such as drought escape, drought avoidance and drought tolerance (Levitt, 1980; Ludlow, 1989; Zhu et al., 2016; Rodrigues et al., 2019). Through tiny microscopic pores in the surface of leaves called stomata, plants assimilate CO_2 for photosynthesis by trading-off water, required for transpiration and other biological processes. This close intimacy between productivity and water use contributes to the adaptation of plants to their growing environments. Therefore, genetic variation in WUE and transpiration efficiency (TE, biomass production/transpirational water loss) that occurs as a result of intentional (via breeding/selection) and unintentional selection in nature provides an opportunity to identify and assemble useful alleles for improving the productivity of various crops.

WUE can be measured at the single leaf level as intrinsic WUE (*i*WUE), defined as the ratio of the photosynthetic CO_2 assimilation rate (A) over transpirational water loss (stomatal conductance, g_{sw}) or as whole-plant vegetative WUE, as the ratio of total dry matter production to total water transpired or as an integrated whole-plant WUE, as the

ratio of biomass or seed yield to evapotranspiration (Farquhar & Richards, 1984; Zhengbin et al., 2011; Leakey et al., 2019; Raman et al., 2019). *i*WUE assessments using the gas-exchange method are very challenging to be accurately performed, particularly in the large breeding populations, as WUE is regulated by a myriad of plant development, physiological, biochemical and molecular networks (Moore et al., 2009; Takahashi et al., 2018). Farquhar and Richards (1984) proposed $\Delta^{13}C$ as a time-integrated surrogate trait for measuring TE both at the single leaf level and at the whole plant level, as C_3 plants discriminate less against ^{13}C during photosynthesis with increased water deficit stress. The negative relationship between WUE and $\Delta^{13}C$ has been verified in *A. thaliana* (Masle et al., 2005) and in some agricultural crop plants (Farquhar et al., 1982; Ehleringer, 1993; Hall et al., 1994; Rebetzke et al., 2008; Des Marais et al., 2014; Raman et al., 2019), with some exceptions where nil or weak associations were observed (Hammer et al., 1997; Monneveux et al., 2007; Devi et al., 2011; Raman et al., 2020b).

Canola, being the second most important oilseed crop grown worldwide with a global production of 75 million tons (FAO STAT, http://www.fao.org/), is often cultivated in arid and semi-arid regions and faces periodic drought. Despite its economic significance to the oilseed industry as well as being an essential rotational crop in agricultural production systems, little research has been conducted on traits contributing to its drought tolerance (McVetty et al., 1989; Knight et al., 1994; Matus et al., 1995; Fletcher et al., 2015; Fletcher et al., 2016; Pater et al., 2017; Hossain et al., 2020; Raman et al., 2020a; Raman et al., 2020b). More recently, it was shown that two canola inbred lines, BC1329 and BC9102 vary by ~ 2‰ in their $\Delta^{13}C$ signatures (Hossain et al., 2020). However, the genetic basis of variation in $\Delta^{13}C$ and other integrated WUE traits such as plant biomass, flowering time and seed yield was not deciphered. Thus, a comprehensive understanding of the genetic and physiological bases underlying WUE is central to developing strategies for resilience to water deficit conditions.

Herein, through comprehensive analyses based on extensive phenotypic and physiological measurements, genetic and genomic studies, we demonstrate that multiple genetic and environmental determinants underlie plasticity in multi-dimensional drought avoidance traits such as $\Delta^{13}C$, early vigour, plant height and seed yield, and drought

escape traits such as flowering time in canola. We also show that one of the QTL for multi-traits; $\Delta^{13}C$, days to flower, plant height and seed yield on chromosome A09 is subjected to homoeologous recombination.

Materials and methods

Plant materials

In total, 223 doubled haploid (DH) lines derived from the F_1 cross between advanced breeding lines 'BC1329' (maternal parent) and 'BC9102' (paternal parent) were utilised for different genetic analysis experiments. An F_2 population comprising 744 lines derived from a single F_1 plant from BC1329/BC9102 was employed for fine mapping/verification of QTL associated with $\Delta^{13}C$.

Phenotypic evaluation for WUE traits

Four experiments were conducted in order to (i) determine the genomic regions that influence the expression of the traits associated with WUE (Experiments 1-3) and (ii) determine the relationship between $\Delta^{13}C$, *i*WUE and integrated WUE related traits under wet and dry conditions (Experiment 4). Experiments 1 and2 were performed under natural field conditions to measure WUE at the plot level; Experiment 3 is a pot experiment for single plant level WUE measurements and Experiment 4 is a rain-out shelter experiment with wet and dry irrigation regimes for measuring WUE at the single leaf level. Details of the experimental designs are presented in Table S4. Monthly weather statistics for average atmospheric temperatures and rainfall are also presented (Fig. S1).

Phenotypic trait measurements

Several agronomic, gas exchange and other physiological traits were measured for genetic analysis. A summary of the experiments in terms of their aim, trial layout, genetic material evaluated, and the traits measured are presented (Table S1, Fig. S2). Details of trait measurements are given in our recent study (Raman et al., 2020b) and summarised in Table S2. A brief description of the traits measured is given below.

Plant development and agronomic traits

$\Delta^{13}C$, flowering time, plant height and seed yield were measured for Experiments 1-4 and normalised difference in the vegetative index (NDVI) was measured only for Experiment 2. $\Delta^{13}C$ was determined from multi-phase experiments with appropriate experimental designs (Smith et al., 2006)) to account for the variations attributed to field/pot and laboratory conditions. The $\delta^{13}C$ composition was determined using Vienna Pee Dee Belemnite (VPDB) as the ultimate reference. $\Delta^{13}C$ was calculated from the $\delta^{13}C$ values assuming the isotopic composition of CO_2 in the air to be -7.8‰ on the VPDB scale, as described previously (Farquhar & Richards, 1984). Fresh and dry weights of the leaf and leaf thickness were also measured from F_2 plants and row plots under wet conditions in Experiment 4.

Physiological traits

The gas exchange measurements were taken at the single leaf level for the plots under wet conditions in Experiment 4, as this relationship varies under different water-deficit levels. We determined *i*WUE by measuring light-saturated assimilation rate (*A*) and stomatal conductance to the diffusion of water vapour (g_{sw}). The 5th fully expanded leaf of each of the 72 lines of BC1329/BC9102 DH population (06-5101DH), including parental lines, was tagged and utilised for gas exchange measurements.

Light microscopy

A leaf disc (9.08 cm^2 size) was taken from each of two replicate canola lines from Experiment 4 (wet block), fixed and stored in 70% ethanol as detailed (Table S4). Leaf sections were stained using a method modified from Rae *et al.* (2020) and were imaged using 488 nm excitation and 500-560 nm emission on a Leica SP8 confocal microscope.

Genotyping and linkage map construction

Genotyping of DH lines was carried-out using the genotyping-by-sequencing (GBS) based DArTseq approach (Raman et al., 2014). Sequence polymorphisms were used for linkage map construction following the method detailed in Raman *et al* (2016). The markers that showed complete segregation between each other were 'binned' into a unique locus and the resulting 'bin' map was used to identify trait-marker associations.

To obtain the physical position of markers, DArTseq sequences were aligned with the Darmor-*bzh* reference assembly version 4.1 using the default parameter settings with the Bowtie program.

Statistical methods

Commensurate with the aims of the experiments and the structure of the data sets, for Experiments 1-3 whole genome, single-step quantitative trait loci (QTL) analyses were performed on each trait using an extension of the approach developed by Verbyla and Cullis (2012) within a multi-environment trial (MET) analysis framework using factor analytic linear mixed models (FA-LMM) (Smith et al., 2015). Whereas, each trait measured on Experiment 4 is analysed individually using appropriate linear mixed models (LMM). A detailed description of the methods is presented (Table S4).

All analyses were performed in *ASReml-R* (Butler et al., 2018), which provides residual maximum likelihood (REML) estimates of variance parameters, empirical best linear unbiased predictions (EBLUPs) of random effects and empirical best linear unbiased estimates (EBLUEs) of fixed effects. The extent of genetic control of traits was investigated by calculating line mean H^2 (broad-sense heritability) as the mean of the squared accuracy of the predicted DH line effects as described previously (Cullis et al., 2006) and found to be dependent on the environment. The across environment summary measure of Overall performance (OP) proposed by Smith and Cullis (2018) was used to identify lines of interest. We examined the relationships of $\Delta^{13}C$ with agronomic traits (seed yield, days to flowering, plant height and NDVI) using pair-wise correlations of Overall performance estimates from the MET analysis of each trait or the EBLUPs from the LMM analysis of each trait.

Identification of candidate genes for WUE

Arabidopsis thaliana genes which had been annotated with various WUE-related terms were retrieved from the TAIR 10 database (https://www.arabidopsis.org/). These genes were then used to identify putative homologues in canola.

Resequencing and structural variation analysis of parental lines

Libraries from high-quality genomic DNA from both parental lines, BC1329 and BC9102, were constructed using the Illumina TruSeq DNA preparation kit, following the manufacturer's instructions (Illumina). Whole-genome resequencing (2 x 150 bp) was performed at the Novogene facility (Novogene Co., Ltd, Hong Kong) using the Illumina HiSeq 2000 sequencing platform. The coverage of the parental lines ranged from 77.6× (BC1329, 102.6 Gb) to 83.8× (BC 9102, 112.4 Gb). Read mapping to the 'Darmor-*bzh*' reference assembly (version 4.1, http://www.genoscope.cns.fr/brassicanapus/data/), SNP and InDel (< 50-bp) calling, structural variation (SV, ≥ 50-bp) detection and identification of HE event (≥ 10-kb windows) was performed as described in Raman *et al.* (2021).

Development of sequence-capture based DArTAg markers

We processed sequence data for target QTL regions on A09 and C09 chromosomes (Table S12) and selected 154 SNPs for DArTag oligo-synthesis. Oligos were synthesised by IDT (Ultramer DNA Oligos, http://idtdna.com) at 200 pmol scale, pooled in the equimolar amount into a single assay and used for processing 8 plates of DNA with the F_2 population and a control canola sample using a proprietary DArTag assay (Targeted Genotyping - Diversity Arrays Technology) using 384 plate format. For each plate, a sample of the pooled product was also run on agarose gel and compared against positive control before proceeding with the sequencing process. The libraries were sequenced on Illumina Hiseq2500 with an average volume of sequencing per sample at 43,225 sequencing reads (median at 46,389) and average read depth per assay at 280. Marker data were extracted using DArT PL's proprietary algorithm deployed a plugin in KDCompute application framework (https://www.kddart.org/kdcompute.html).

RNA sequencing and differential gene expression analysis

Parental lines, BC1329 and BC9102 of DH population were grown in three replicates under both wet (100% field capacity) and dry (50% field capacity) treatments in a glasshouse (Table S4). The clean sequence reads (100 bp single-end reads) for 12 samples that had per base sequence quality with >96% bases above Q30 were aligned against the *B. napus* reference Darmor-*bzh* (Version 4.1), using STAR aligner (v2.5.3a) (https://github.com/alexdobin/STAR/blob/master/doc/STARmanual.pdf). The raw

counts of reads mapping to each known gene was used to perform differential expression analysis using edgeR (version 3.30.3) (https://bioconductor.org/packages/release/bioc/html/edgeR.html) using R version 4.0.3. A generalised linear model approach was then used to quantify the differential expression between the groups. The differentially expressed genes (DEGs) were obtained using a false discovery rate (FDR < 0.05). Heatmaps showing the expression pattern of genes in A09 and C09 QTL regions were produced using the ComplexHeatmap R package (Gu et al., 2016).

Results

Substantial genetic variation in $\Delta^{13}C$ and other WUE traits

We observed high levels of genetic variation in $\Delta^{13}C$ and other WUE related traits in the DH mapping population. The significant source of genetic variation was from the additive component (genetic markers), which ranged from 21.5% for NDVI to 79.1% for days to flower (Table S5, Additive M1, %). Broad sense heritability estimates for $\Delta^{13}C$ and other integrated WUE related traits (plant height, NDVI, flowering time and seed yield) were variable, ranging from low (56%) to high (98%), depending on the nature of trait and growing environment (Table S6). Estimated additive and total (additive plus non-additive) genetic correlations between environments revealed that there are strong correlations between environments for both additive and total genetic variance with values greater than 0.89 and 0.83, respectively, for all traits (Table S7). Overall performance estimates for $\Delta^{13}C$ ranged from 18.73 to 21.25‰ and displayed transgressive segregation among DH lines across phenotypic environments (Fig. 1a, Table S8). Up to 2.52‰ variation in $\Delta^{13}C$ was observed among DH lines that equates to a 5-fold increase compared with the parental lines.

Relationships between WUE traits at plot level

To determine the relationships between $\Delta^{13}C$ and other WUE related traits, pair-wise correlations were obtained using the genotype Overall Performance estimates across environments (Fig. 1b). The $\Delta^{13}C$ showed a negative correlation with days to flower (r = - 0.58), while positive correlations were observed with NDVI, a proxy for plant vigour (r = 0.37), plant height (r = 0.45) and seed yield (r = 0.59). Flowering time showed a negative correlation with seed yield (r = - 0.63). The promising DH lines that had high

296 WUE of yield (high $\Delta^{13}C$) for use in canola breeding programs based on the Overall
297 performance estimates are presented in Fig. 1c. DH line 06-5101-137 had the maximum
298 $\Delta^{13}C$ (21.25‰) among the DH progenies.
299
300 Relationships between physiological WUE (single leaf level) and integrated WUE
301 (whole plant level)
302 Significant variation for both *A* and g_{sw} was observed, although H^2 estimate of *i*WUE
303 was low (Table S9). This may have occurred due to variable VPD across gas exchange
304 measurements during the experiment, highlighting the plasticity of *i*WUE and $\Delta^{13}C$ as
305 traits. Genotype EBLUPs for *A* and g_{sw} ranged from 4.97 to 17.15, and 0.11 to 0.38,
306 respectively (Table S9). Pairwise correlations revealed that both *A* and g_{sw} are dependent
307 on each other with a correlation of 0.56 (Fig. 2a). We observed a negative correlation
308 between $\Delta^{13}C$ and *iWUE* (r = - 0.16), indicating that DH lines with low $\Delta^{13}C$ have
309 higher *iWUE*, consistent with the findings made earlier (Farquhar & Richards, 1984). There
310 was a more negative correlation between *iWUE* and g_{sw} (r = - 0.46) in comparison to *A*
311 (r = -0.27), suggesting that g_{sw} is the predominant driver for variation in *i*WUE
312 parameters.

313 This study showed that $\Delta^{13}C$ correlates negatively with *i*WUE but it ($\Delta^{13}C$) correlates
314 positively with seed yield (Fig. 2a). Under well-watered conditions, there were negative
315 correlations between $\Delta^{13}C$ and days to flower, *A* and *iWUE*. We further investigated
316 relationships between leaf water content (LWC) at a single leaf level and WUE traits at
317 the whole plant level and found that LWC show a negative relationship with $\Delta^{13}C$, but it
318 did not show any relationship with seed yield (Fig. 2a). Further, the estimated genetic
319 correlations between wet and dry blocks for seed yield (Fig. 2b) and plant height, the
320 only two traits measured after imposing water stress at the first flowering stage, were
321 very high (0.93 for both traits). This suggests that genotype by irrigation block
322 interaction is small. High $\Delta^{13}C$ lines revealed higher yield across irrigation blocks
323 compared to low $\Delta^{13}C$ lines.

324

325 Genetic basis underlying $\Delta^{13}C$ and WUE related traits

We constructed a linkage map that includes 8,985 DArTseq markers onto 24 linkage groups (LGs), representing all the 19 chromosomes of *B. napus* (Table S10). To reduce computation time for genetic analysis, we produce a 'bin' map of 1793 markers that spanned a total of 1965.29 cM, with an average interval of 1.10 cM between adjacent loci.

Multi-environment QTL analysis identified a total of 29 QTL (15 QTL for main-effects and 14 for QTL (Q) × Environment (E) interactions) for variation in $\Delta^{13}C$ and other WUE related traits (Table 1, Table S11). For leaf $\Delta^{13}C$, three QTL main effects that showed statistically significant (LOD ≥3) associations were identified on chromosomes A08, A09 and C09, while one 'suggestive' QTL (LOD >2.5 but less than 3) was located on chromosome A07 (Table 1, Fig. 3a). We identified QTL for phenotypic plasticity in different traits between three growing environments (Q × E effects) on A02, A05, A08, A09, A10, C02, C03, C06, C07 and C09 chromosomes (Table S11). For $\Delta^{13}C$ plasticity, two QTL were identified on chromosomes A02 and C06, although the size of allelic effects were environment-dependent (Table S11). Collectively, QTL explained 38% of genotypic variation in $\Delta^{13}C$ (Table S5, VAF_m).

Comparative localisation of QTL

Three QTL for multi-traits on chromosomes A01, A08 and A09 were colocalised to the same genomic regions (Table 1). One QTL delimited with marker 3153720 for variation in $\Delta^{13}C$ was colocated with days to flower, plant height and seed yield on chromosome A09 (Table 1, Fig. 3a). We further sought a correlation between allelic effects of markers and variation in $\Delta^{13}C$, days to flower, plant height and seed yield (Fig. 3b-e). Up to 68% of allelic effects were explained by the same marker allele (Fig. 3e), suggesting pleiotropic relationships between these traits and/or tight genetic linkage between them.

Verification of QTL for $\Delta^{13}C$

We validated the genetic control, the linkage between DArTseq markers and $\Delta^{13}C$ (in DH population) and focused on the identification of candidate gene(s) underlying the majority of genetic variation in $\Delta^{13}C$ at QTL regions on chromosomes A09 and C09

(Table 1). The $\Delta^{13}C$ values showed a wide range distribution among F_2 lines (Fig. 4a). Unlike DH lines, $\Delta^{13}C$ exhibited a positive correlation with flowering time and LWC, and a negative correlation with SLW (Fig. 4b-d). Our anatomical analysis of leaf discs that revealed both parental lines BC1329 and BC9102 differ in thickness and arrangement of palisade and spongy mesophyll cells: BC1329 (192 μm) had high porosity with large airspaces compared to BC9102 (184 μm, Fig. 4e-f), which may facilitate gas exchange, thus leading to efficient water use.

Genetic analysis revealed that several DArTag markers show significant segregation distortion (deviating from the normal segregation consistent with 1:2:1 ratio for codominance, or 3:1 ratio for dominance) on chromosomes A09 and C09 (Table S12), suggesting that the $\Delta^{13}C$ region could be subjected to structural variation. Genome scan using linear marker regression revealed that DArTag markers positioned at 28,598,612 bp on chromosome A09, and 46318271 bp on C09 of the Darmor-*bzh* genome exhibit statistically significant association with $\Delta^{13}C$ variation (Fig. S3).

Physical mapping and candidate genes associated with WUE near $\Delta^{13}C$ QTL

To identify potential candidate genes involved in the $\Delta^{13}C$ variation, we interrogated genomic regions underlying the significantly associated markers in both the mapping (DH) and validation populations (F_2). In the DH population, DArTseq 3153720 'bin' marker revealed the complete linkage with another 12 markers, which were localised within 1.49 Mb region, spanning 28.35 Mb to 29.35 Mb (Table S10, Fig. S3). Annotation of genomic interval revealed that several genes including *ERECTA* (BnaA09g40540D), *PYL2* (BnaA09g40690D), *H^+ATPase-5* (BnaA09g41340), *LEA18* (BnaA09g42180D) and *Protein Kinase* (BnaA09g42220D) on chromosome A09 and on its homoeologous chromosome C08, and *HAC11* (BnaC09g46960D), floral repressor *FLC (FLC.C09a*; *BnaC09g46500* and *FLC.C09b*; *BnaC09g46540D*), Myc-type BHLH (BnaC09g46950D, BnaC09g47080D on homoeologous group C09/A10 chromosomes are likely candidates to be involved in $\Delta^{13}C$ variation (Table S13, Fig. S3). DArTag marker (physical position on the Darmor-*bzh* genome: 28,598,612 bp) on chromosome A09 was located within 93 kb of the *ERECTA* gene that controls transpiration efficiency in *A. thaliana* (Masle et al., 2005).

388 $\Delta^{13}C$ QTL region on chromosome A09 is subjected to homoeologous exchange (HE)

389 We observed significant segregation distortion among marker alleles on chromosomes
390 A09 and C09 in both mapping (DH) and validation (F_2) populations and inconsistency in
391 collinearity across both genetic and physical maps (Table S12). To investigate whether
392 QTL region on A09 is subjected to structural variation**,** we performed HE analysis
393 utilising resequencing data of the parental lines. Sequence mapping revealed 26 genomic
394 regions undergone HE events, varying from 90 kb to 870 kb, including the A09 multi-
395 trait QTL region (29.3 to 29.5 Mb), BC9102 from C08 chromosome, as a result of
396 homoeologous recombination (Fig. 5a, Table S14). However, in the maternal line
397 BC1329**,** no such event was identified (Fig. 5b).

398

399 Gene expression changes for $\Delta^{13}C$ variation in the A09 and C09 QTL intervals between
400 the parents

401 To investigate the expression of candidate genes that underlie the $\Delta^{13}C$ variation on
402 chromosomes A09 and C09, we examined the leaf tissue-specific transcriptome of the
403 two parental lines: BC1329 and BC9102 under wet and dry conditions. We found that a
404 total of 60 genes on A09 and 51 genes on C09 underlying $\Delta^{13}C$ QTL regions were
405 significanty differentially expressed between the two parental lines (Table S15). Of the
406 DEGs, several of them such as Casein Kinase 2 α4 (BnaA09g42220D), Cation-
407 transporting P-type ATPase (BnaA09g41340D, BnaA09g42040D), BEL1-like
408 homeodomain protein 4 (BnaA09g41850D), Spermidine disinapoyl acyltransferase
409 (BnaA09g41960D), Protein Kinase (BnaA09g42220D, BnaA09g41970D), HEC3
410 (BnaC09g46950D), and serine carboxypeptidase (BnaC09g47000D), are related with
411 water use, water use efficiency and response to water stress
412 (https://www.arabidopsis.org/). We also found that the expression levels of genes in
413 BC9102 (with HE event) such as BnaA09g41850D, BnaA09g41970D (wall-associated
414 receptor kinase-like 14), BnaA09g41990D (cyclin-dependent kinase inhibitor),
415 BnaA09g42000D (nicotinate phosphoribosyltransferase 2), BnaA09g42030D (RNA
416 recognition motif domain), and BnaA09g42040D were significantly higher (at least 2-
417 fold) than those of BC1329 (without HE event) (Fig. 6, Table S15), suggesting that HE
418 may be responsible for expression variation at the $\Delta^{13}C$-QTL region on A09.

419

DISCUSSION

Canola reveals considerable variation for $\Delta^{13}C$

We found substantial genotypic variation in $\Delta^{13}C$, from 18.78 to 21.23‰ among DH, and 20.9 to 27.2‰ among F_2 lines. An earlier study has shown that an increase of 0.5‰ in $\delta^{13}C$ can lead to 25% more transpiration efficiency (TE = biomass gained/water transpired) in *Arabidopsis* (Juenger et al., 2005). Extrapolating this relationship, which is positive between $\delta^{13}C$ and TE, and negative between $\Delta^{13}C$ and TE, canola F_2 lines with 6.3‰ higher $\Delta^{13}C$ values than parental lines (22.8 to 23.5‰) should reduce WUE theoretically by 315%, which is impossible. It reflects the dependence of the sensitivity on the general level of $\Delta^{13}C$. For example, Masle et al. (2005) found that at the level they saw in *Arabidopsis*, an increase in $\Delta^{13}C$ of 1‰ was associated with a 15% decrease in TE. Previous studies revealed that canola lines display a range of variation in $\Delta^{13}C$ (18.7 to 23.7‰). Triazine tolerant (TT) accessions show higher $\Delta^{13}C$ values compared to conventional open-pollinated varieties and hybrids (Matus et al., 1995; Pater et al., 2017; Hossain et al., 2020; Raman et al., 2020b). In this study, we utilised non-TT accessions for genetic analysis. Our research thus provides an additional genetic resource for understanding the genetic and physiological basis, as well as improving WUE in canola.

Integrated WUE is partly driven by fitness traits

This study showed that DH lines that discriminate less between ^{12}C and ^{13}C as carbon source for photosynthesis (low $\Delta^{13}C$) show higher *i*WUE at the single leaf level (Fig. 2a). However, low Δ^{13} lines did not produce high yield (agronomic WUE; seed yield/unit of water used at the whole plot level) suggesting that selection for low *i*WUE at a single leaf level is useful for improving seed yield (r = 0.34, Fig. 2a), rather than using low $\Delta^{13}C$ as a surrogate trait for predicting high seed yield in canola, consistent with our earlier findings (Raman et al., 2020b). This inconsistent relationship between $\Delta^{13}C$ and seed yield could be due to genotypic variation in WUE being driven by variation in water use rather than by variation in assimilation per unit of water applied (Kobata et al., 1996; Blum, 2005; Sinclair, 2018). WUE, being a multi- dimensional trait can also be driven with other 'fitness' traits that reduce evapo-transpiration rate and crop water use. For example, high $\Delta^{13}C$ lines with faster growth (NDVI, a proxy for plant

vigour and plant height) could provide quicker canopy cover, which enables plants to reduce water loss from soil evaporation, thus increasing seed yield (r = 0.45 to 0.72, Fig. 1b). This is partly supported by in this study showing high correlation between plant fitness and seed yield and tight linkage of corresponding QTL (Fig. 1-3). In addition, $\Delta^{13}C$ exhibited negative correlations with flowering time (r= - 0.58; DH population), and a positive correlation with NDVI, plant height and seed yield (Fig. 1b), suggesting that high $\Delta^{13}C$ lines tend to 'escape' via accelerating growth and flowering - an evolutionary trait for adaptation to terminal drought stress. Our results showed that genotypes with low $\Delta^{13}C$ had less canopy cover, late flowering and lower seed yield; these characteristics are typical for plants with drought avoidance strategy (TE). However, under terminal water-deficit situations, low $\Delta^{13}C$ lines could yield poorly due to the shorter seed filling period, accompanied with high temperatures. It remains to establish how low $\Delta^{13}C$ lines which require a longer season for seed filling, perform in climates that are not prone to environmental constraints (non-water deficit/heat stress).

Genetic and environmental determinants affect phenotypic trait expression

We observed plasticity between $\Delta^{13}C$, and flowering time evaluated under field/pot and rain-out shelter (negative correlation, Fig. 1b, 2A) but a positive correlation under glasshouse conditions (Fig. 4b). This could be due to growing conditions (non- water stress condition, 100% field capacity) and nature of leaf tissue (discs without much vascular tissue) analysed for $\Delta^{13}C$.

Our comprehensive multi-environment QTL analysis showed that by using well-designed multiphase experiments (Table S3), and efficient statistical models (Table S4), both genetic and environmental determinants underpinning phenotypic variation can be deciphered for traits of interest (Table S11). For example, we identified QTL for the main effects (on A01, A07, A08 and A09) and Q x E interaction effects (on A02 and C06) that describe $\Delta^{13}C$ plasticity across different environments (Table S11). Multi-environment based QTL analysis is a more powerful approach to dissect complex traits than the traditional QTL approaches (Zhang et al., 2010) but it was not used to uncover the genetic basis of WUE traits in canola previously. Consistent detection of $\Delta^{13}C$-QTL across three environments suggests that these loci contribute to the adaptive capacity of

DH lines to water-deficit stress conditions and thus translating to economic seed yield (~1 t/ha). Across field environments, DH lines were subjected to water deficit conditions, right from stem elongation to seed maturity (rainfall ranged from 225 to 235 mm over seven months of growing season, Fig. S2). Colocation of QTL for seed yield, $\Delta^{13}C$ and plant height at the same genomic regions and stable allele (BC9102), contributing to trait variation that suggest multi-trait QTL on chromosome A09 are associated with effective water use. Early flowering showed a negative relationship with seed yield (Table 1), reiterating crosstalk between drought stress signalling and flowering time pathways (Des Marais et al., 2012).

It was interesting that none of the $\Delta^{13}C$ QTL that we identified for main effect and Q x E interactions (Table S11) were detected in the Skipton/Ag-Spectrum population (Raman et al., 2020b). In an independent study, Mekonnen *et al.*, (2020) identified three QTL for $\delta^{13}C$ on chromosomes A02, A09, and C08 in the North American *B. napus* mapping population. However, none of the QTL were consistently detected across environments. It is yet to establish whether the genomic region on chromosome A09 or its homoeologous counterpart C08 (QTL for root pulling force, plant height and $\delta^{13}C$) is the same as found in our study, as the authors did not report the physical positions of QTL marker-intervals. In addition, there was a poor marker coverage on chromosome C08 in our genetic mapping population (13 markers, Table S10), which may have led to QTL (if any) being undetected in the unmapped regions, especially in HE region. These studies suggest that several genomic regions on A02, A03, A07, A09, C03, C06, C08, and C09 control variation in $\Delta^{13}C$, thus, genetic architecture of $\Delta^{13}C$ is rather complex.

A priori genes regulating WUE and efficient water use underlie QTL for $\Delta^{13}C$

Coarse and high-resolution mapping approaches utilised herein facilitated the validation of genomic regions for Δ^{13} variation and delimited candidate genes in canola, which are implicated in leaf-level WUE (Hersen et al., 2008; Cutler et al., 2010; Youn et al., 2016; Tao et al., 2018; Menéndez et al., 2019). For example, this study identified and validated a QTL that influences multiple traits; $\Delta^{13}C$, days to flower, plant height and seed yield on chromosome A09 that map within 92 kb of the *ERECTA* gene (Table S13). In different plant species, *ERECTA* and *ERECTA Like 1,2* genes encoding leucine-rich repeat protein

514 kinases, regulate stomatal density and patterning, inflorescence architecture, ovule
515 development, transpiration, and thermo-tolerance (Torii et al., 1996; Godiard et al., 2003;
516 Shpak et al., 2003; Masle et al., 2005; Meng et al., 2012; Pillitteri & Torii, 2012; Bemis et al.,
517 2013; Shen et al., 2015; Guo et al., 2020). *ERECTA* is also shown to control spikelet
518 number- a component trait of grain yield via crosstalk between a Mitogen-activated
519 protein kinase (MAPK) signalling pathway and cytokinin metabolism in rice. However,
520 we did not find any difference in the level of expression of *ERECTA* between parental
521 lines differing in Δ^{13} (unpublished data). We also localised several stress-responsive
522 genes, including DEGs that may contribute to drought avoidance strategies via signal
523 transduction pathways, encoding functional proteins (LEA18, RD20, glycine
524 metabolism, CAT) and regulatory proteins, including transcription factors (bHLH,
525 MYB, TINY2, ATHB6), protein kinases (Tyrosine protein kinase, Wall-associated
526 receptor kinase-like 14, MAPK, SNF1-related protein kinase) and receptors (ABA
527 receptor PYL12), phosphatases (PP2C), and calmodulins (CPK17) (Jonak et al., 2002; Des
528 Marais et al., 2014; Jagodzik et al., 2018; Yong et al., 2019) within QTL intervals associated
529 with Δ^{13}C variation (Table 1, Table S13, S15). Plant expressing PYL12, and SRK2C
530 genes are shown to improve the water use and drought tolerance (Yang et al., 2016)
531 whereas ABC transporter (ABCG22) and ABA responsive kinase gene, MPK12 reduced
532 the WUE (Des Marais et al., 2014). Our data hint that genes affecting stomatal
533 characteristics (RD20, ERECTA), leaf thickness and water-deficit responsive genes
534 described above likely underlie WUE and drought avoidance traits, while Q x E
535 interactions are likely driven by environmental cues (PHYTOCHROME C was mapped
536 with 6.2 kb from Δ^{13}C-QTL on C06, Table S13).

537 Our results suggest that a QTL region underlying Δ^{13}C, flowering time, plant height and
538 seed yield on chromosome A09 may be subjected to HE. Homoeologous recombination
539 is associated with presence-absence variation (Nicolas et al., 2007; Hurgobin et al., 2018).
540 Recently, a major QTL for homoeologous recombination, *BnaPh1* was mapped on A09
541 (Higgins et al., 2021) and this was located within 5 Mbp of the QTL region that is
542 associated with multiple traits. It is possible that the same genomic region may be
543 involved in regulating WUE in diverse canola accessions and require further research.

In summary, this current study demonstrates that measures of *i*WUE, $\Delta^{13}C$ and integrated WUE are complex and modulated by environmental and genetic determinants, including those subject to homoeologous exchange. Our findings on identification of useful variation in $\Delta^{13}C$ (up to 6.3‰) and its underlying basis of variation in WUE traits, including their plasticity across environments, and identification of favourable alleles for increasing WUE would provide potential resources for developing new drought tolerant varieties for drier-environments to continue making genetic gains in the breeding programs.

Sequence data availability

The raw sequence data reported in this paper has been deposited in the National Center for Biotechnology Information Sequence Read Archive (Accession no. PRJNA743730 for RNA-Seq data, PRJNA743989 for whole-genome resequencing data).

Acknowledgements

This study was supported by the Australian Grains Research and Development Corporation and NSW Department of Primary Industries and partners (projects: DAN00117, and DAN00208. We thank Dr Simon Diffey (Apex Biometry) for multi-phase experimental designs for $\Delta^{13}C$ and Dr. Alison Smith (UOW) for constructive discussions on the statistical methods.The authors are grateful to Mr. Warren Bartlett and Mr. Dean McCullum, for their assistance in sowing and management of field experiments; Hannah Roe and Wayne Pitt for grinding leaf samples for $\Delta^{13}C$ analysis and Advanta for providing F_1 cross.

Author contributions

HR designed research; HR, RR, BM and YQ, performed field experiments; HSW analysed samples for carbon isotope discrimination; BC developed the statistical methods; RP, YZ, NS, HR, and SL analysed data; HR, NS, AZ and AK developed DArTags; BM, HR and GF performed/interpreted gas exchange measurements; RW investigated microscopic analysis; AE and DT provided seeds of F_1; HR prepared manuscript with inputs from others. All authors read and approved this manuscript for publication.

575

576 # Reference

577

578 **Bemis SM, Lee JS, Shpak ED, Tori KU. 2013.** Regulation of floral patterning and organ identity
579 by Arabidopsis ERECTA-family receptor kinase genes. *Journal of Experimental Botany,*
580 *Vol. 64, No. 17, pp. 5323–5333, doi:10.1093/jxb/ert270*
581 **Bertolino LT, Caine RS, Gray JE. 2019.** Impact of stomatal density and morphology on water-
582 use efficiency in a changing world. *Front Plant Sci* **10**: 225.
583 **Blum A. 2005.** Drought resistance, water-use efficiency, and yield potential—Are they
584 compatible, dissonant or mutually exclusive? Aust. J. Agr. Res. 56:1159–1168.
585 **Blum A. 2009.** Effective use of water (EUW) and not water-use efficiency (WUE) is the target of
586 crop yield improvement under drought stress. Field Crops Research 112, 119–123.
587 **Butler DG, Cullis BR, Gilmour AR, Gogel BJ, Thompson R. 2018.** ASReml-R Reference Manual
588 Version 4. Technical report, VSN International Ltd, Hemel Hempstead, HP1 1ES, UK.
589 **Cullis BR, Smith AB, Coombes NE. 2006.** On the design of early generation variety trials with
590 correlated data. *Journal of Agricultural, Biological, and Environmental Statistics 11,*
591 *381–393. doi: 10.1198/108571106X154443*.
592 **Cutler SR, Rodriguez PL, Finkelstein RR, Abrams SR. 2010.** Abscisic Acid: Emergence of a Core
593 Signaling Network. *Annual Review of Plant Biology* **61**(1): 651-679.
594 **Des Marais DL, Auchincloss LC, Sukamtoh E, McKay JK, Logan T, Richards JH, Juenger TE. 2014.**
595 Variation in *MPK12* affects water use efficiency in Arabidopsis and reveals a pleiotropic
596 link between guard cell size and ABA response. *Proc Natl Acad Sci U S A* **111**(7): 2836-
597 2841.
598 **Des Marais DL, McKay JK, Richards JH, Sen S, Wayne T, Juenger TE. 2012.** Physiological
599 genomics of response to soil drying in diverse Arabidopsis accessions. *Plant Cell* **24**(3):
600 893-914.
601 **Devi MJ, Bhatnagar-Mathur P, Sharma KK, Serraj R, Anwar SY, Vadez V. 2011.** Relationships
602 between transpiration efficiency and its surrogate traits in the rd29A:DREB1A
603 transgenic lines of groundnut. *Journal of Agronomy and Crop Science* **197**(4): 272-283.
604 **Ehleringer JR. 1993.** Gas-exchange implications of isotopic variation in arid-land plants. In H
605 Griffiths, J Smith, eds, Plant Responses to Water Deficit. BIOS Scientific Publishers,
606 London, pp 265–284.
607 **Farquhar GD, O'Leary MH, Berry JA. 1982.** On the relationship between carbon isotope
608 discrimination and intercellular carbon diooxide concentration in leaves. *Aust. J. Plant*
609 *Physiol.* **9**: 121-137.
610 **Farquhar GD, Richards RA. 1984.** Isotopic composition of plant carbon correlates with water-
611 use efficiency of wheat genotypes. Australian Journal of Plant Physiology 11, 539–552.
612 **Fletcher RS, Herrmann D, Mullen JL, Li Q, Schrider DR, Price N, Lin J, Grogan K, Kern A, McKay**
613 **JK. 2016.** Identification of polymorphisms associated with drought adaptation QTL in
614 *Brassica napus* by resequencing. *G3: Genes|Genomes|Genetics* **6**(4): 793-803.
615 **Fletcher RS, Mullen JL, Heiliger A, McKay JK. 2015.** QTL analysis of root morphology, flowering
616 time, and yield reveals trade-offs in response to drought in *Brassica napus*. *Journal of*
617 *Experimental Botany* **66**(1): 245–256, https://doi.org/210.1093/jxb/eru1423.
618 **Gleick PH. 2000.** Ed., In: The world water 2000-2001: The Biennial Report on Freshwater
619 Resources (Island Press, 2000). p 53.
620 **Godiard L, Sauviac L, Torii KU, Grenon O, Mangin B, Grimsley NH, Marco Y. 2003.** ERECTA, an
621 LRR receptor-like kinase protein controlling development pleiotropically affects
622 resistance to bacterial wilt. *Plant J* **36**(3): 353-365.

Gu Z, Eils R, Schlesner M. 2016. Complex heatmaps reveal patterns and correlations in multidimensional genomic data. *Bioinformatics* **32**(18): 2847-2849.

Guo T, Lu Z-Q, Shan J-X, Ye W-W, Dong N-Q, Lin H-X. 2020. *ERECTA1* acts upstream of the OsMKKK10-OsMKK4-OsMPK6 cascade to control spikelet number by regulating cytokinin metabolism in rice. *The Plant Cell*: tpc.00351.02020.

Hall AE, Richards RA, Condon AG, Wright GC, Farquhar GD. 1994. Carbon isotope discrimination and plant breeding. *Plant Breed. Rev. 12, 81–113*.

Hammer GL, Farquhar GD, Broad IJ. 1997. On the extent of genetic variation for transpiration efficiency in sorghum. *Australian Journal of Agricultural Research* **48**(5): 649-656.

Hersen P, McClean MN, Mahadevan L, Ramanathan S. 2008. Signal processing by the HOG MAP kinase pathway. *Proceedings of the National Academy of Sciences* **105**(20): 7165-7170.

Higgins EE, Howell EC, Armstrong SJ, Parkin IAP. 2021. A major quantitative trait locus on chromosome A9, *BnaPh1*, controls homoeologous recombination in *Brassica napus*. *New Phytologist* **229**(6): 3281-3293.

Hossain SM, Masle J, Easton A, Hunter MN, Godwin ID, Farquhar GD, Lambrides CJ. 2020. Genetic variation for leaf carbon isotope discrimination and its association with transpiration efficiency in canola (*Brassica napus*). *Funct Plant Biol* **47**(4): 355-367.

Hurgobin B, Golicz AA, Bayer PE, Chan C-KK, Tirnaz S, Dolatabadian A, Schiessl SV, Samans B, Montenegro JD, Parkin IAP, et al. 2018. Homoeologous exchange is a major cause of gene presence/absence variation in the amphidiploid *Brassica napus*. *Plant biotechnology journal* **16**(7): 1265-1274.

Jagodzik P, Tajdel-Zielinska M, Ciesla A, Marczak M, Ludwikow A. 2018. Mitogen-Activated Protein Kinase cascades in plant hormone signaling. *Front Plant Sci* **9**: 1387.

Jonak C, Okrész L, Bögre L, Hirt H. 2002. Complexity, cross talk and integration of plant MAP kinase signalling. *Curr Opin Plant Biol* **5**(5): 415-424.

Juenger TE, McKay JK, Hausmann N, Keurentjes JJB, Sen S, Stowe KA, Dawson TE, Simms EL, Richards JH. 2005. Identification and characterization of QTL underlying whole-plant physiology in *Arabidopsis thaliana*: δ13C, stomatal conductance and transpiration efficiency. *Plant, Cell & Environment* **28**(6): 697-708.

Kijne JW, Barker R, (Eds.) MD. 2003. Water productivity in agriculture: limits and opportunities for improvement. *Wallingford, UK: CABI; Colombo, Sri Lanka: International Water Management Institute (IWMI). xix, 332p. (Comprehensive Assessment of Water Management in Agriculture Series 1)*.

Knight JD, Livingston NJ, Van Kessel C. 1994. Carbon isotope discrimination and water-use efficiency of six crops grown under wet and dryland conditions. *Plant, Cell & Environment* **17**(2): 173-179.

Kobata T, Okuno T, Yamamoto T. 1996. Contributions of capacity for soil water extraction and water use efficiency to maintenance of dry matter production in rice subjected to drought. *Japanese Journal of Crop Science, 65(4), 652-662.* https://doi.org/10.1626/jcs.65.652.

Koohafkan P, Stewart BA. 2008. Water and Cereals in Dryland. *The Food and Agriculture Organisation of the United Nations and Earthscan, London, Sterling, VA*.

Leakey ADB, Ferguson JN, Pignon CP, Wu A, Jin Z, Hammer GL, Lobell DB. 2019. Water use efficiency as a constraint and target for improving the resilience and productivity of c3 and c4 crops. *Annual Review of Plant Biology* **70**(1): 781-808.

Levitt J. 1980. Responses of plants to environmental stresses. Volume II. Water, Radiation, Salt, and Other Stresses. Academic Press, New York.

671 **Ludlow MM. 1989.** Strategies in response to water stress, p. 269–281. In: H.K. Kreeb, H.
672 Richter, and T.M. Hinkley (eds.). Structural and functional response to environmental
673 stresses: Water shortage. SPB Academic Press, The Netherlands.
674 **Masle J, Gilmore SR, Farquhar GD. 2005.** The *ERECTA* gene regulates plant transpiration
675 efficiency in Arabidopsis. *Nature* **436**(7052): 866-870.
676 **Matus A, Slinkard A, van Kessel C. 1995.** Carbon isotope discrimination: Potential for indirect
677 selection for seed yield in canola. *Crop Sci.* **35**(5): 1267-1271.
678 **McVetty PBE, Austin RB, Morgan CL. 1989.** A comparison of the growth, photosynthesis,
679 stomatal conductance and water use efficiency of *Moricandia* and *Brassica* species *Ann.*
680 *Bot.* **64**: 87-94.
681 **Mekonnen MD, Mullen JL, Arathi HS, Assefa Y, McKay JK, Byrne PF. 2020.** Quantitative trait
682 locus mapping for carbon isotope ratio and root pulling force in canola. *Agrosystems,*
683 *Geosciences & Environment* **3**(1): e20095.
684 **Menéndez AB, Calzadilla PI, Sansberro PA, Espasandin FD, Gazquez A, Bordenave CD, Maiale**
685 **SJ, Rodríguez AA, Maguire VG, Campestre MP, et al. 2019.** Polyamines and legumes:
686 joint stories of stress, nitrogen fixation and environment. *Frontiers in Plant Science*
687 **10**(1415).
688 **Meng X, Wang H, He Y, Liu Y, Walker JC, Torii KU, Zhang S. 2012.** A MAPK cascade downstream
689 of ERECTA receptor-like protein kinase regulates arabidopsis inflorescence architecture
690 by promoting localized cell proliferation. *The Plant Cell* **24**(12): 4948-4960.
691 **Mills G, Sharps K, Simpson D, Pleijel H, Frei M, Burkey K, Emberson L, Uddling J, Broberg M,**
692 **Feng Z, et al. 2018.** Closing the global ozone yield gap: Quantification and cobenefits
693 for multistress tolerance. *Global Change Biology* **24**(10): 4869-4893.
694 **Monneveux P, Sheshshayee MS, Akhter J, Ribaut J-M. 2007.** Using carbon isotope
695 discrimination to select maize (Zea mays L.) inbred lines and hybrids for drought
696 tolerance. *Plant Science* **173**(4): 390-396.
697 **Moore JP, Le NT, Brandt WF, Driouich A, Farrant JM. 2009.** Towards a systems-based
698 understanding of plant desiccation tolerance. *Trends Plant Sci* **14**(2): 110-117.
699 **Nicolas SD, Mignon GL, Eber F, Coriton O, Monod H, Clouet V, Huteau V, Lostanlen A,**
700 **Delourme R, Chalhoub B, et al. 2007.** Homeologous recombination plays a major role
701 in chromosome rearrangements that occur during meiosis of *Brassica napus* haploids.
702 *Genetics* **175**(2): 487-503.
703 **Passioura JB. 1977.** Grain yield, harvest index and water use of wheat. J. Aust. Inst.Agric. Sci.
704 43, 117–121.
705 **Pater D, Mullen JL, McKay JK, Schroeder JI. 2017.** Screening for natural variation in water use
706 efficiency traits in a diversity set of brassica napus l. identifies candidate variants in
707 photosynthetic assimilation. *Plant Cell Physiol* **58**(10): 1700-1709.
708 **Pillitteri LJ, Torii KU. 2012.** Mechanisms of stomatal development. *Annu Rev Plant Biol* **63**: 591-
709 614.
710 **Rae AE, Wei X, Flores-Rodriguez N, McCurdy DW, Collings DA. 2020.** Super-resolution
711 fluorescence imaging of *Arabidopsis thaliana* transfer cell wall ingrowths using pseudo-
712 Schiff labelling adapted for the use of different dyes. *Plant and Cell Physiology 61:*
713 *1775–1787.*
714 **Raman H, Raman R, Kilian A, Detering F, Carling J, Coombes N, Diffey S, Kadkol G, Edwards D,**
715 **McCully M, et al. 2014.** Genome-wide delineation of natural variation for pod shatter
716 resistance in *Brassica napus. PLoS ONE 9(7): e101673.*
717 *https://doi.org/10.1371/journal.pone.0101673* **9**(7): e101673.
718 **Raman H, Raman R, Mathews K, Diffey S, Salisbury P. 2020a.** QTL mapping reveals genomic
719 regions for yield based on an incremental tolerance index to drought stress and related

agronomic traits in canola. *Crop and Pasture Science 71(6) 562-577* https://doi.org/10.1071/CP20046.

Raman H, Raman R, McVittie B, Borg L, Diffey S, Yadav AS, Balasubramanian S, Farquhar GD. 2020b. The genetic and physiological basis for phenotypic variation in effective water use in *Brassica napus Food and Energy Security.* https://doi.org/10.1002/fes3.237.

Raman H, Raman R, Qiu Y, Zhang Y, Batley J, Liu S. 2021. The *Rlm13* gene, a new player of *Brassica napus-Leptosphaeria maculans* interaction maps on chromosome C03 in canola *Front. Plant Sci. | doi: 10.3389/fpls.2021.654604*.

Raman H, Uppal RK, Raman R 2019. Genetic solutions to improve resilience of canola to climate change. In: Kole C ed. *Genomic Designing of Climate-Smart Oilseed Crops*. Cham: Springer International Publishing, 75-131.

Raman R, Diffey S, Carling J, Cowley R, Kilian A, Luckett D, Raman H. 2016. Quantitative genetic analysis of yield in an Australian *Brassica napus* doubled haploid population. *Crop & Pasture Science* **67**(4): 298-307.

Rebetzke GJ, Condon AG, Farquhar GD, Appels R, Richards RA. 2008. Quantitative trait loci for carbon isotope discrimination are repeatable across environments and wheat mapping populations. *Theor Appl Genet* **118**(1): 123-137.

Rodrigues J, Inzé D, Nelissen H, Saibo NJM. 2019. Source–Sink Regulation in Crops under Water Deficit. *Trends in Plant Science* **24**(7): 652-663.

Shen H, Zhong X, Zhao F, Wang Y, Yan B, Li Q, Chen G, Mao B, Wang J, Li Y, et al. 2015. Overexpression of receptor-like kinase ERECTA improves thermotolerance in rice and tomato. *Nat Biotechnol* **33**(9): 996-1003.

Shpak ED, Lakeman MB, Torii KU. 2003. Dominant-negative receptor uncovers redundancy in the Arabidopsis ERECTA Leucine-rich repeat receptor-like kinase signaling pathway that regulates organ shape. *Plant Cell* **15**(5): 1095-1110.

Sinclair TR. 2018. Effective water use required for improving crop growth rather than transpiration efficiency. *Frontiers in Plant Science* **9**(1442).

Smith A, Ganesalingam A, Kuchel H, Cullis B. 2015. Factor analytic mixed models for the provision of grower information from national crop variety testing programmes. *Theoretical and Applied Genetics 128:55–72.*

Smith A, Lim P, Cullis B. 2006. The design and analysis of multi-phase plant breeding experiments. *Journal of Agricultural Science 144* **5**: 393-409.

Smith AB, Cullis BR. 2018. Plant breeding selection tools built on factor analytic mixed models for multi-environment trial data. *Euphytica 214(8), 143.* https://doi.org/10.1007/s10681-018-2220-5.

Smith S, De Smet I. 2012. Root system architecture: insights from *Arabidopsis* and cereal crops. *Philosophical Transactions of the Royal Society B: Biological Sciences* **367**(1595): 1441-1452.

Takahashi F, Kuromori T, Sato H, Shinozaki K. 2018. Regulatory gene networks in drought stress responses and resistance in plants. *Adv Exp Med Biol.* **1081:189-214**.

Tao Y, Chen M, Shu Y, Zhu Y, Wang S, Huang L, Yu X, Wang Z, Qian P, Gu W, et al. 2018. Identification and functional characterization of a novel BEL1-LIKE homeobox transcription factor GmBLH4 in soybean. *Plant Cell, Tissue and Organ Culture (PCTOC)* **134**(2): 331-344.

Torii KU, Mitsukawa N, Oosumi T, Matsuura Y, Yokoyama R, Whittier RF, Komeda Y. 1996. The Arabidopsis ERECTA gene encodes a putative receptor protein kinase with extracellular leucine-rich repeats. *The Plant Cell* **8**(4): 735-746.

Verbyla AP, Cullis BR. 2012. Multivariate whole genome average interval mapping: QTL analysis for multiple traits and/or environments. *Theoretical and Applied Genetics 125, 933–953.* https://doi.org/10.1007/s00122-012-1884-9.

770 **Yang Z, Liu J, Tischer SV, Christmann A, Windisch W, Schnyder H, Grill E. 2016.** Leveraging
771 abscisic acid receptors for efficient water use in *Arabidopsis*. *Proceedings of the*
772 *National Academy of Sciences* **113**(24): 6791-6796.
773 **Yong Y, Zhang Y, Lyu Y. 2019.** A MYB-related transcription factor from *Lilium lancifolium L.*
774 *(LlMYB3)* is involved in anthocyanin biosynthesis pathway and enhances multiple
775 abiotic stress tolerance in *Arabidopsis thaliana*. *Int J Mol Sci* **20**(13).
776 **Youn H-S, Kim TG, Kim M-K, Kang GB, Kang JY, Lee J-G, An JY, Park KR, Lee Yj, Im YJ, et al.**
777 **2016.** Structural insights into the quaternary catalytic mechanism of hexameric human
778 quinolinate phosphoribosyltransferase, a key enzyme in de novo NAD biosynthesis.
779 *Scientific Reports* **6**(1): 19681.
780 **Zhang Y, Li Y-x, Wang Y, Liu Z-z, Liu C, Peng B, Tan W-w, Wang D, Shi Y-s, Sun B-c, et al. 2010.**
781 Stability of QTL across environments and QTL-by-environment interactions for plant
782 and ear height in maize. *Agricultural Sciences in China* **9**(10): 1400-1412.
783 **Zhengbin Z, Ping X, Hongbo S, Mengjun L, Zhenyan F, Liye C. 2011.** Advances and prospects:
784 biotechnologically improving crop water use efficiency. *Crit Rev Biotechnol* **31**(3): 281-
785 293.
786 **Zhu M, Monroe JG, Suhail Y, Villiers F, Mullen J, Pater D, Hauser F, Jeon BW, Bader JS, Kwak**
787 **JM, et al. 2016.** Molecular and systems approaches towards drought-tolerant canola
788 crops. *New Phytol* **210**(4): 1169-1189.

789

Legends of Figures

Fig. 1: Genetic variation in WUE traits and their relationships among doubled haploid lines derived from the cross, BC1329/BC9102. **a:** Frequency distribution of the Overall performance estimates for $\Delta^{13}C$. Estimates for the parental lines are shown with arrows; **b:** Pair-wise correlations of the Overall performance estimates between $\Delta^{13}C$ (‰) and other WUE related traits; **c:** Top four DH lines that showed the highest $\Delta^{13}C$ based on Overall performance estimates across environments in relation to control commercial varieties of canola and the parental lines are shown.

Fig. 2: Relationships between $\Delta^{13}C$, gas exchange measurements (CO_2 assimilation (A), stomatal conductance (g_{sw}), and intrinsic water use efficiency (*i*WUE), plant developmental and agronomic traits (LWC: leaf water content; DTF: Days to flower; PH: Plant height and SY: Seed yield) of selected 70 DH lines of the BC1329/BC9102 population, representing extremes (High and low values) in $\Delta^{13}C$ and their parents. **a:** Pair-wise correlations of the genotype EBLUPs are plotted. DH lines were grown under rain-out shelter with wet and dry conditions. **b**: Relationships between $\Delta^{13}C$ and seed yield for wet and dry blocks. Genotype EBLUPs for $\Delta^{13}C$ and seed yield are plotted. Parental lines and the DH lines with high and low $\Delta^{13}C$ are labelled.

Fig. 3: Distribution and relationships between Overall performance estimates of $\Delta^{13}C$, days to flower (DTF), plant height (PH) and seed yield (SY) and DArTseq marker alleles for the QTL (3153720) that colocalized in the same genomic region on chromosome A09. Manhattan plot showing LOD scores for associations between DArTseq markers and $\Delta^{13}C$ (a). QTL main effects are labelled with the respective trait (for days to flower, plant height and seed yield only the 3153720 QTL is shown) and QTL x Environment interactions are labelled with the trait followed by 'Q × E' (only shown for $\Delta^{13}C$). LOD scores presented in the Manhattan plot are from the genome scan for the QTL main effects where the LOD scores of the significant QTL are replaced with the ones from the final model. The black dash line indicates the threshold value for significant SNPs at LOD ≥ 3. Box plots showing the distribution of the Overall performance estimates for $\Delta^{13}C$, days to flower, plant height and seed yield partitioned

into allele combinations, 'AA (BC1329)' and 'BB (BC9102)', for the SNP marker 3153720 (**b**). Pair-wise correlations of Overall performance estimates between $\Delta^{13}C$ vs days to flower (**c**), $\Delta^{13}C$ vs plant height (**d**) and $\Delta^{13}C$ vs seed yield (**e**) are partitioned into different allelic combinations.

Fig. 4: Distribution and relationships of the traits measured for an F_2 validation population derived from the BC1329/BC9102, grown under non-stress conditions. The frequency distribution of $\Delta^{13}C$ (‰) among 744 F_2 lines (**a**). Pair-wise correlations between $\Delta^{13}C$ and DTF (**b**), $\Delta^{13}C$ and LWC (**c**) and $\Delta^{13}C$ and SLW (**d**) are shown. $\Delta^{13}C$: Carbon isotope discrimination; DTF: Days to flower; LWC: Leaf water content; SLW: Specific leaf weight. Leaf sections showing differences in air spaces (AS, marked with arrow) between parental lines BC1329 (**e**) and BC9102 (**f**). EP: epidermis; PM: palisade mesophyll (comparatively regular elongated cells); SM: spongy mesophyll (irregular cells)

Fig. 5: Homoeologous exchange (HE) events detected between parental lines of doubled haploid population derived from the BC1329/BC9102. Genomic sequences that undergone HE are shown in Table S14. Substituted and 'translocated' reads are highlighted in Blue and Red colour, respectively.

Fig. 6: Expression profiles of differentially expressed genes (DEGs) in A09 (a) and C09 9b) QTL regions under water-deficit and water non-deficit conditions of the parental lines of the doubled haploid population derived from the BC1329/BC9102. The normalised read counts were plotted as a heatmap and genes were clustered according to the basis of their expression pattern. The genes in the heatmap were subjected to homoeologous exchange (HE) as well as the genes map within QTL region for $\Delta^{13}C$. DEGs that map within HE regions are highlighted in green boxes.

Table 1: Quantitative trait loci (main effects) for carbon isotope discrimination ($\Delta^{13}C$) and agronomic traits (DTF: Days to flower; NDVI: Normalised difference vegetative difference; PH: Plant height; SY: Seed yield) evaluated in doubled haploid lines from BC1329/BC9102, across three environments. LOD scores, allelic effect, parental allele and percentage of genetic variance explained (R^2) were also provided. QTL x Environment interactions for each environment are presented in supplementary Table S11. Putative candidate genes underlying QTL x Environment interactions are given in Table S13. Suggestive QTL having LOD ≤3 are in italics whereas consistent markers that were associated with multiple traits are in bold font.

Trait	**Marker**	**Chromosome**	**Physical map position of 'Top' marker on Darmor-*bzh* genome version 4.1**	**LOD**	***R*^{2} (%)**	**Allelic effect**	**Parental allele**	**Physical distance from putative candidate genes (Kb) within LD block**
NDVI	*3117901|F|0-11:T>C-11:T>C*	*A01*	*2276244*	*2.79*	*5.87*	*0.02*	*BC1329*	*Tyrosine-protein kinase-BnaA01g04900D* (3.15) *ASP5-BnaA01g04910D* (0.19)
SY	27390647|F|0-42:G>A-42:G>A	A01	3895510	4.17	8.37	-0.06	BC9102	Pentatricopeptide repeat-BnaA01g08190D (1.67) RmlC-like cupins-

								BnaA01g08200D (0.09)
DTF	**4106850|F|0-28:G>A-28:G>A**	**A01**	**3911345**	**4.18**	**12.73**	**1.27**	**BC1329**	**RmlC-like cupins-BnaA01g08210D (3.87) AMT1;4-BnaA01g08220D (7.33)**
PH	**4106850|F|0-28:G>A-28:G>A**	**A01**	**3911345**	**4.54**	**11**	**-2.64**	**BC9102**	
$\Delta^{13}C$	*3098654|F|0-12:G>A-12:G>A*	*A07*	*10641571*	*2.76*	*7.46*	*-0.09*	***BC9102***	*Auxin responsive SAUR protein-BnaA07g11440D (6.09)* *Dehydrin-BnaA07g11450D (0.68)*
PH	**3190876|F|0-10:T>A-10:T>A**	**A08**	**11767812**	**6.77**	**8.7**	**3.34**	**BC1329**	**SAM dependent carboxyl methyltransferase - BnaA08g13630D (0.61)**
SY	**3190876|F|0-10:T>A-10:T>A**	**A08**	**11767812**	**4.84**	**10.76**	**0.06**	**BC1329**	**Tetratricopeptide repeat-BnaA08g13640D (2.17)** **Rab-GTPase-TBC domain-BnaA08g13650D (16.35)**

								Tyrosine-protein kinase-BnaA08g13660D (19.12)
$\Delta^{13}C$	3087427|F|0-17:C>G-17:C>G	A08	13909331	4.57	10.86	0.14	BC1329	Tyrosine-protein kinase-BnaA08g17440D (7.75) Kelch-type beta propeller-BnaA08g17450D (2.73)
DTF	**3153720**	**A09**	**29356333**	**3.01**	**11.84**	**1.04**	**BC1329**	**LEA18-BnaA09g42180D (10.08) SDR3-BnaA09g42190D (5.64)** **Tyrosine-protein kinase-BnaA09g42220D (4.61)** **Embryo-specific 3-BnaA09g42230D (9.32)** **ACA7-BnaA09g42240D (17.43)**
$\Delta^{13}C$	**3153720**	**A09**	**29356333**	**9.57**	**21.3**	**-0.19**	**BC9102**	
PH	**3153720**	**A09**	**29356333**	**6.91**	**10.09**	**-3.36**	**BC9102**	
SY	**3153720**	**A09**	**29356333**	**3.87**	**7.73**	**-0.05**	**BC9102**	
DTF	*3148204|F|0-11:A>G-11:A>G*	*A10*	*12591509*	*2.87*	*15.32*	*-1.08*	*BC910*	*NAD(P)-binding Rossmann-fold superfamily protein-*

							2	*BnaA10g16630D (1.10)* *UTP- BnaA10g16640D (0.52)* *Protein Kinase-BnaA10g16650D (5.20)* *GDH1- BnaA10g16660D (10.53)*
DTF	*4333486*	*C02*	*2170435*	*2.57*	*5.96*	*-0.92*	*BC910 2*	*CYSTATIN - BnaC02g04270D (2.35)* *CLT3 - BnaC02g04280D (2.31)* *CPK17- BnaC02g04290D (2.83)* *Non-haem dioxygenase N-terminal domain-BnaC02g04300D (10.09)* *DGS1- BnaC02g04310D (12.88)*
NDVI	3140998|F|0-9:A>G-9:A>G	C06	18209584	4.46	7.27	0.03	BC132 9	Armadillo-type fold-BnaC06g15500D (8.07) OMR1-BnaC06g15510D (22.46)

SY	27246553	C06	35071983	6.33	8.81	0.07	BC1329	GDSL-like lipase-BnaC06g36590D (11.75) SKP1-BnaC06g36600D (5.06) Galactose oxidase-BnaC06g36610D (3.40) Hap15-BnaC06g36630D (3.03)
PH	*3147080*	*C07*	*30323351*	*2.36*	*3.66*	*2.41*	*BC1329*	*Lipase-BnaC07g23920D (2.28)* *VH1-interacting kinase - BnaC07g23950D (28.05)*
DTF	*5053011|F|0-62:G>A-62:G>A*	*C08*	*22278532*	*2.06*	*7.12*	*-0.88*	*BC9102*	*CYCB2;3- BnaC08g19340D (23.99)* *SUMO- BnaC08g19350D (8.55)* *CAT3- BnaC08g19360D (2.48)* *RWP-RK- BnaC08g19370D (15.01)*

								Tyrosine-protein kinase-BnaC08g19380D (27.23)
$\Delta^{13}C$	3158874	C09	46623311	6.57	18.51	-0.17	BC9102	Hydroxyproline-rich glycoprotein- BnaC09g47070D (6.48) Myc-type, basic helix-loop-helix (bHLH)- BnaC09g47080D (0.72) Phosphate-induced protein 1-BnaC09g47090D (3.74) Epoxide hydrolase-like, alpha/beta-hydrolase-BnaC09g47100D (20.30)
DTF	3152507	C09_ran	3981494	4.21	14.02	1.39	BC1329	TIP1-BnaC09g54140D (0.45) Fatty acid synthase-BnaC09g54150D (10.95)

857

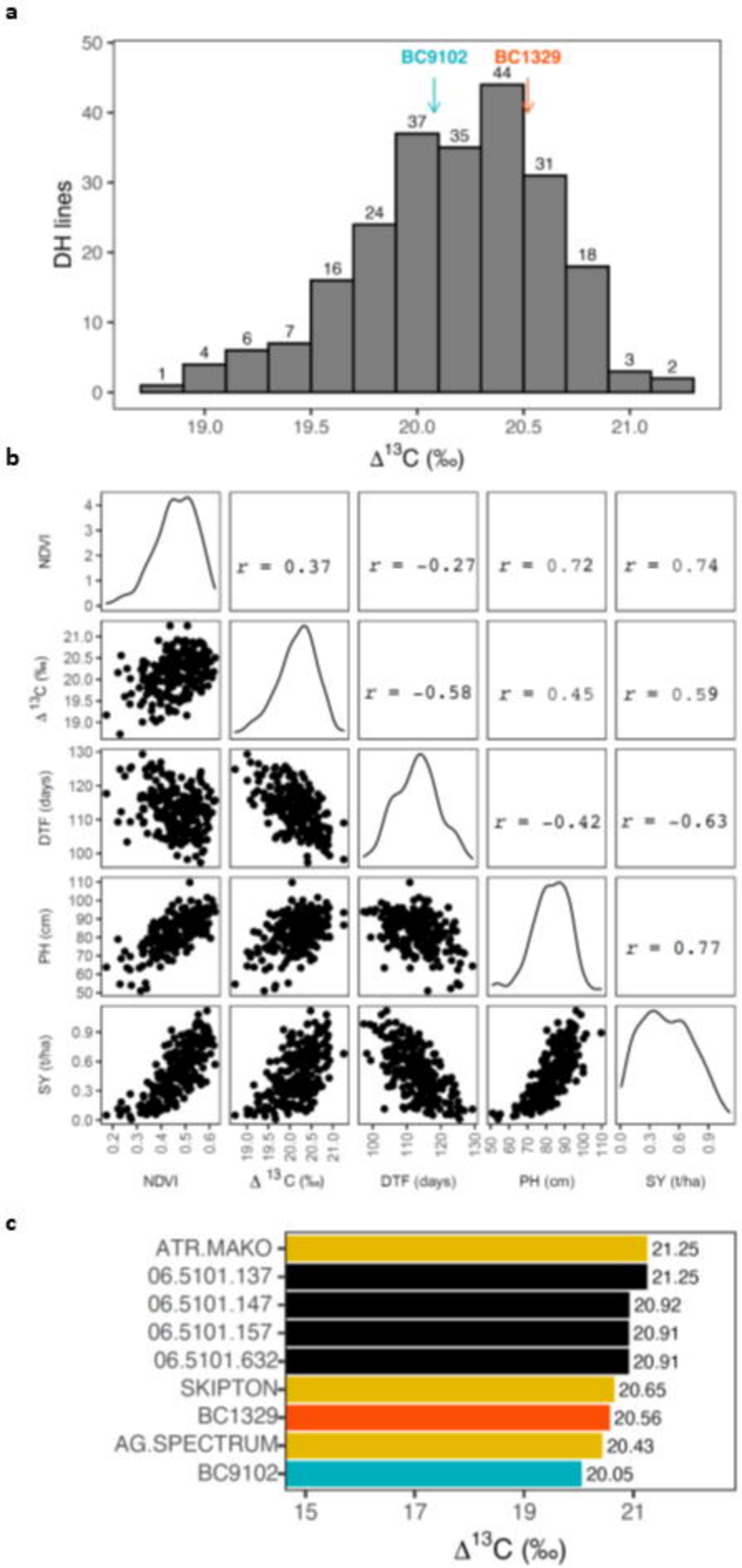

Fig. 1

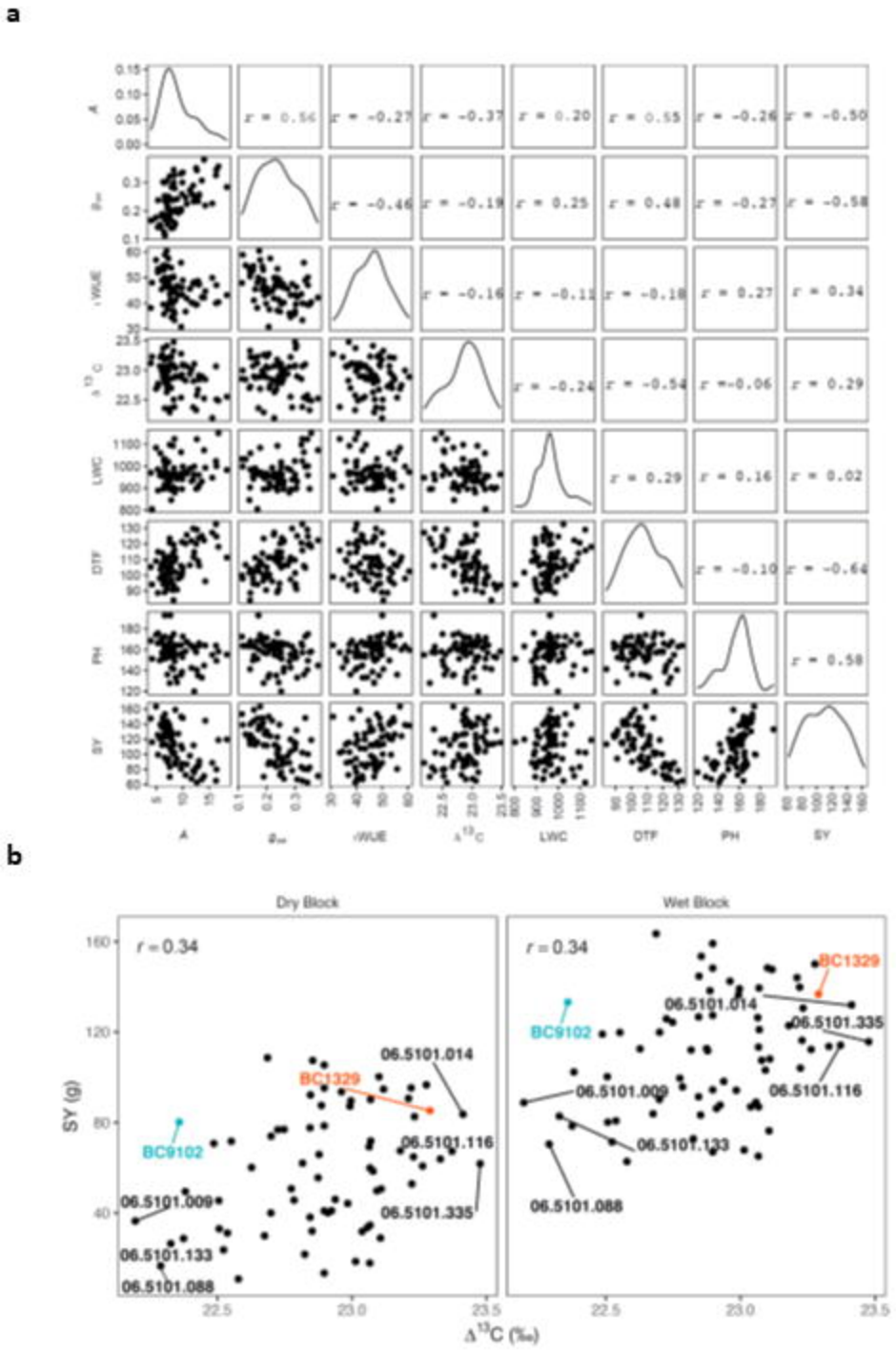

Fig. 2

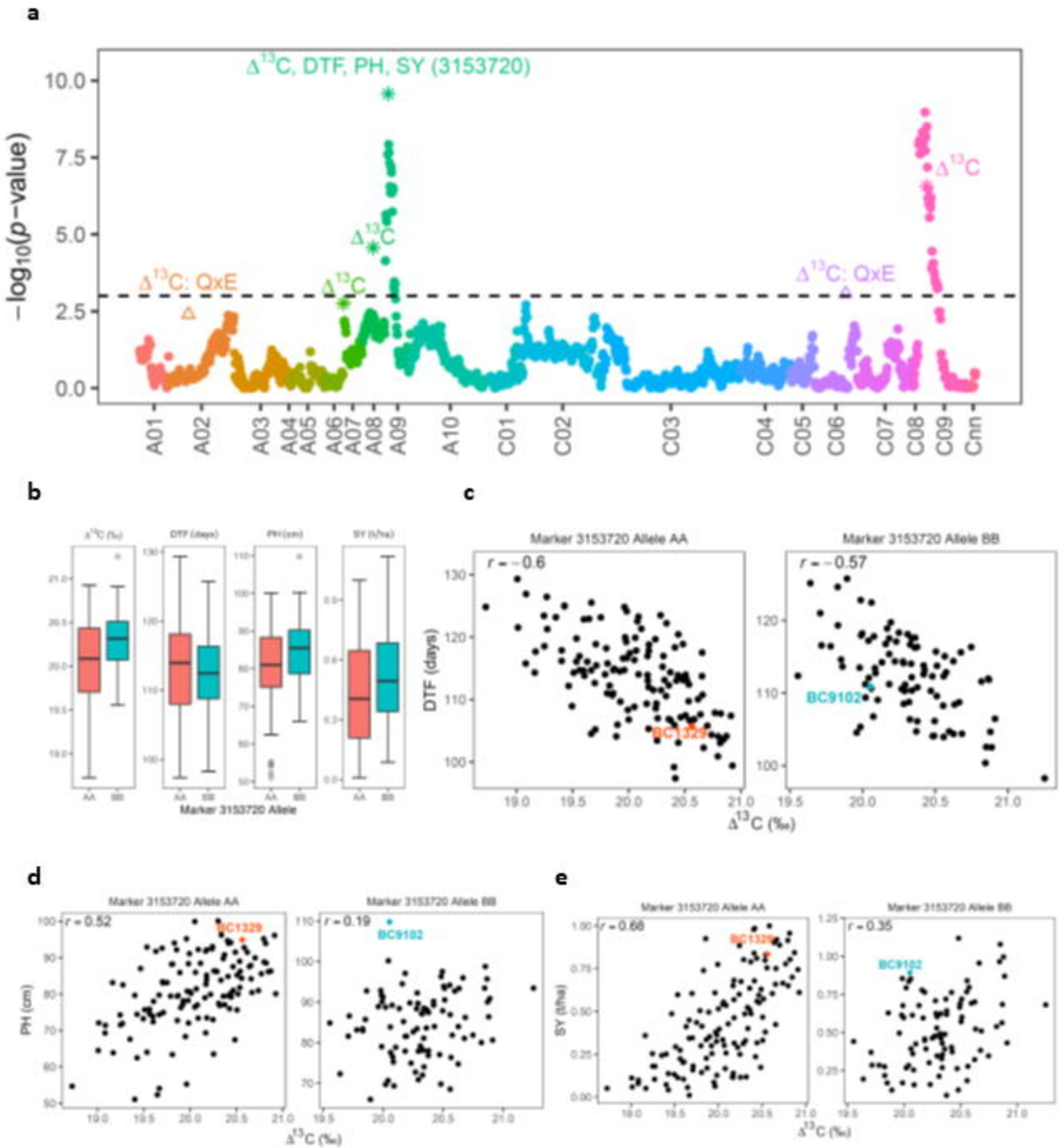

Fig. 3

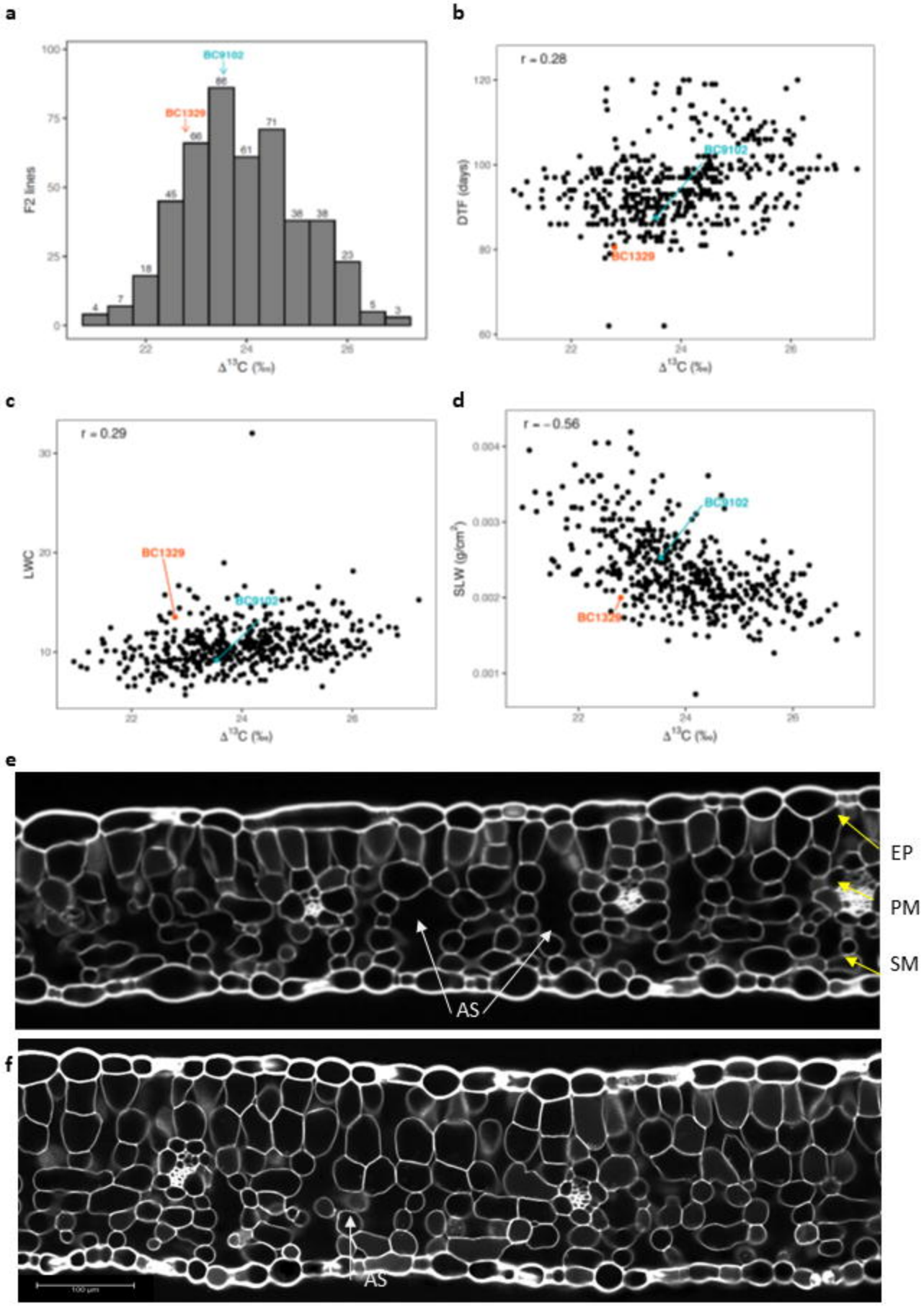

Fig. 4

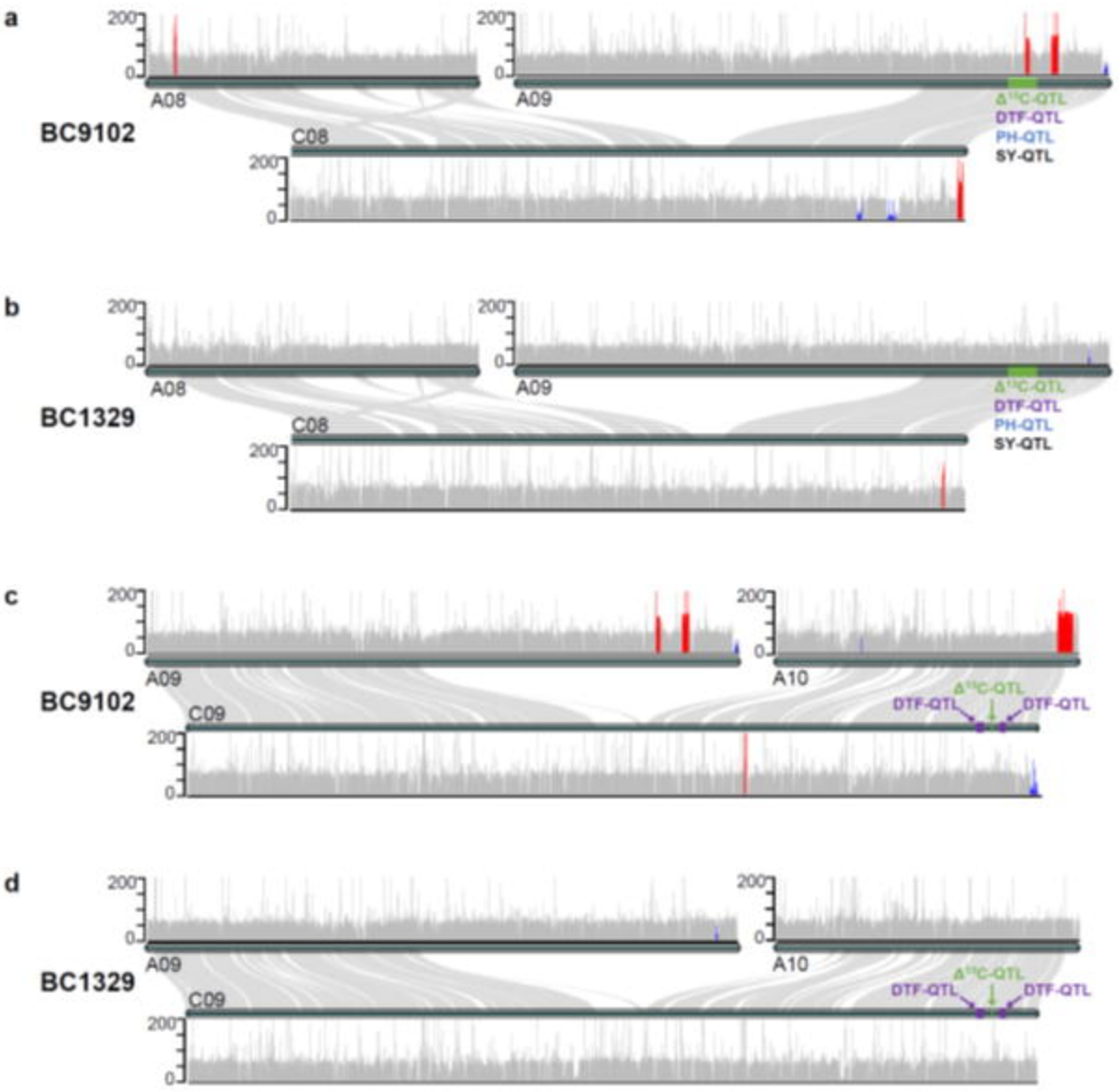

Fig. 5

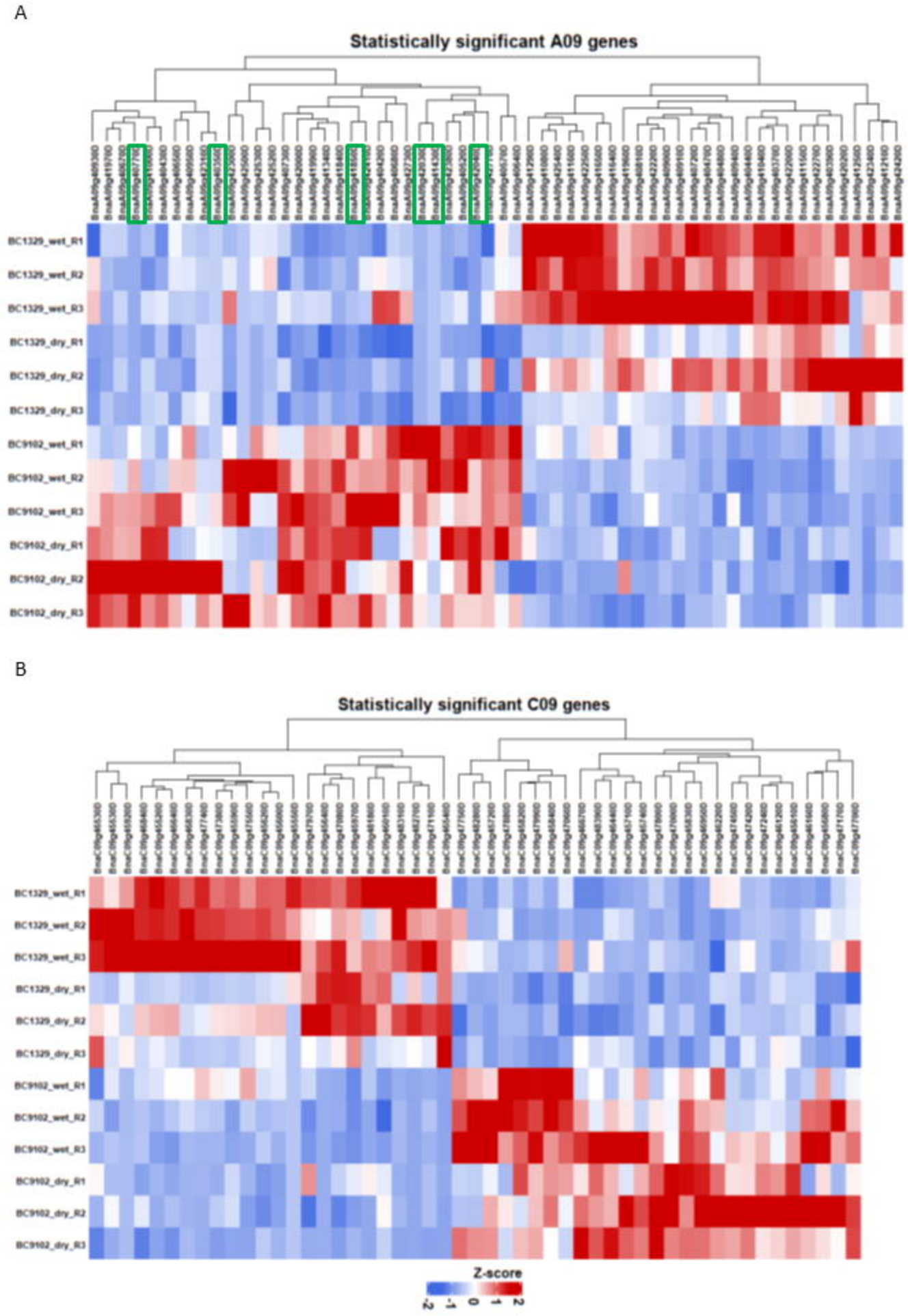

Fig. 6